Astron. Astrophys. 168, 17–24 (1986)

ASTRONOMY
AND
ASTROPHYSICS

Investigation of a complete sample of flat spectrum radio sources from the S5 Survey

I. Analysis

A. Eckart[1,4], A. Witzel[1], P. Biermann[1], K.J. Johnston[2], R. Simon[2], C. Schalinski[1], H. Kühr[3]

[1] Max-Planck-Institut für Radioastronomie, Auf dem Hügel 69, D-5300 Bonn[1], Federal Republic of Germany
[2] E.O. Hulburt Center for Space Research, Naval Research Laboratory, Washington D.C., USA
[3] Max-Planck-Institut für Astronomie, D-6900 Heidelberg, Federal Republic of Germany
[4] Steward Observatory, Univ. of Arizona, Tucson, USA

Received October 10, accepted December 16, 1985

Summary. Thirteen extragalactic sources that fulfil the following criteria 1) declination $\geq 70°$ and galactic latitude $|b^{II}| \geq 10°$, 2) 5 GHz flux density ≥ 1 Jy, and 3) spectral index between 2.7 and 5 GHz ≥ -0.5 ($S \sim \nu^{+\alpha}$) were mapped with high angular resolution (milliarcseconds) at 1.6 and 5 GHz by means of *VLBI*. Initial measurements at 10.6 and 22.2 GHz for four sources are also reported. With the achieved dynamic ranges of $\sim 50:1$ the sources display one to at least nine components on the milliarcsecond scale.

The core components of all the sources are self-absorbed at 1.6 GHz with a median spectral index $\alpha_5^{1.6}$ of 0.4 ± 0.2 while the secondary components have a median spectral index of -0.7 ± 0.3 and display lower flux densities than the cores at all frequencies above 1.6 GHz. Comparison of the measured to the predicted X-ray flux density of the core radio components indicates that all sources should display bulk relativistic motion with small angles to the line of sight and thus the probability of displaying superluminal motion is very high for these sources. There are four new candidates for superluminal motion (0212 + 73, 1150 + 81, 1928 + 73, 2007 + 77) among these 13 sources, as indicated by rapid changes in their radio structures.

In this paper we present the analysis of the survey whereas the maps and most of the tabular material are presented in Eckart *et al.*, 1986 (Paper II).

Key words: quasars: general – BL Lacertae objects – surveys interferometry

1. Introduction

In order to study the physics of compact extragalactic radio sources we are carrying out a detailed investigation of a complete sample of flat spectrum objects over a large range of wavelengths (from the radio to X-rays) and resolutions (from arcseconds, in some cases even arcminutes, to milliarcseconds).

The motivation for this work is to obtain statistically meaningful data to eventually answer the following questions: a) what fraction of active galactic nuclei show the effect of relativistic beaming? b) what is the physical nature of the "relativistic jets" and their emission knots? c) what is the physical mechanism that accelerates the electrons which radiate in the various knots of a "relativistic jet"?

The sources were selected from the fifth installment of the MPIfR-NRAO 5 GHz strong source surveys (Kühr *et al.*, 1981). The selection criteria were as follows:

1) $\delta \geq 70°$, $|b^{II}| \geq 10°$
2) S (4990 MHz) ≥ 1 Jy at the epoch of the survey
3) α (2.7, 5 GHz) ≥ -0.5 ($S \sim \nu^{+\alpha}$)

These criteria were fulfilled by 13 objects listed in Table 1. Their optical identification revealed 7 QSOs and 6 BL Lac type objects. First results on the milliarcsecond (mas) structures of the sample have been given by Eckart *el al.*, (1982) and by Eckart and Witzel (1983). Some preliminary results of the X-ray, optical and radio observations have been discussed by Biermann *et al.* (1981; 1982) and Johnston *et al.* (1984). In this paper we present the results of high resolution radio observations of the selected sources at (up to) four wavelengths, including the results of repeated 6 cm observations of 8 members of the sample as well as optical and X-ray observations.

2. The observations

2.1. The optical observations

Optical data for the thirteen S5 sources which meet the criteria given in the introduction are listed in Table 1. In column (1) we give the names of the radio sources, and in column (2) and (3) the 1950.0 positions for their optical counterparts. These were determined on Palomar Observatory Sky Survey (POSS) prints, using a PDS microdensitometer; the positional r.m.s. uncertainties are expected to be on the order of 0.6 arcsec. The positions agree with accurate radio positions which are given in Witzel and Johnston (1982).

In column (4) the optical identifications are classified as "QSO" (optical emission lines present), or as "BL" (BL Lac type object with featureless optical continuum and significant optical polarization, e.g. $P > 5\%$). Estimated optical magnitudes from the POSS prints are listed in column (5), which are uncertain by about 0.5 mag. Emission line redshifts are presented in column

Send offprint requests to: A. Witzel

Table 1. Optical data for the complete sample

Source	RA (1950)	Dec (1950)	Ident.	m_v	z[a]	P (%)[a]	$[\theta]$
S5 0016 + 73	00 16 54.11	+73 10 51.3	QSO	18.0	1.76		
S5 0153 + 74	01 53 04.01	+74 28 05.8	QSO	16.0	2.34		
S5 0212 + 73	02 12 49.93	+73 35 40.5	BL	19.0		7.8 ± 1.9	96.8 ± 7.1
S5 0454 + 84	04 54 57.34	+84 27 53.7	BL	16.5	cont	18.5 ± 2.2	49.8 ± 3.4
S5 0615 + 82	06 15 32.74	+82 03 56.4	QSO	17.5	0.71		
S5 0716 + 71	07 16 12.93	+71 26 15.1	BL	13.2	cont	13.9 ± 1.2	11.1 ± 2.4
S5 0836 + 71	08 36 21.56	+71 04 22.1	QSO	16.5	2.16		
S5 1039 + 81	10 39 27.79	+81 10 23.4	QSO	16.5	1.26		
S5 1150 + 81	11 50 23.70	+81 15 10.6	QSO	18.5	1.25		
S4 1749 + 70[b]	17 49 03.43	+70 06 39.1	BL	16.5	0.76?		
S5 1803 + 78	18 03 39.24	+78 27 54.8	BL	16.4	cont	35.2 ± 0.4	96.2 ± 0.3
S5 1928 + 73	19 28 49.38	+73 51 45.1	QSO	15.5	0.36		
S5 2007 + 77	20 07 20.55	+77 43 58.2	BL	16.7	cont	15.1 ± 0.9	87.4 ± 1.7

[a] Redshifts, spectral information, and optical polarization data taken from Biermann *et al.* (1981), and Kühr *et al.* (1986b)

[b] The optical position was taken from Crane, and Price (1976), a finding chart is given there, too. A redshift was suggested by Arp *et al.* (1976)

(6) and are accurate to the 1% level; the detection of a featureless optical spectrum is indicated by "cont.".

The optical polarization measurements appear in column (7) and (8). The polarimetric and spectroscopic observations have been carried out at the Steward Observatory 2.3-m-telescope. During repeated observations the "BL"s showed a high degree of variability.

Finding charts for the optical counterparts were prepared and are given elsewhere (Kühr *et al.*, 1986a).

2.2. VLBI observations and data reduction

The observations were carried out over a period of four years from 1979 to 1983 using the facilities of the European and United States VLB Networks. In addition we used the following non-network stations: NRL and Crimea (see Table 2). A summary of the individual sources, experiments etc. is given in Paper II. Here we give a brief summary of the method of observation. The observations were carried out at 18, 6, 2.8, 1.3 cm wavelength, and the data were correlated at the Max-Planck-Institut für Radioastronomie in Bonn. For the observations below 1.3 cm wavelength the Mk II *VLBI* system with a bandwidth of 2 MHz (Clark, 1973) was used. At 1.3 cm the Mk III *VLBI* system (Mode *B*, bandwidth: 28 MHz, Rogers *et al.*, 1983) was used.

Table 2 summarizes the epochs, frequencies, bandwidths, stations, and the observed sources along with comments on the observing mode used in the different experiments. In almost all experiments two or more sources were alternated with scan lengths of 15 to 20 min. This allowed observations of a large number of sources with a dense u-v coverage and enabled correction for possible pointing errors through comparison of the visibilities of the two sources.

In all cases where we had a sufficient number of measurements (more than 80 to 100 measurements spread over the u-v plane) the data were initially mapped at the MPI using the standard data reduction techniques using closure phases and calibrated amplitudes. The starting model was a point source in all cases. Typically about 5–10 iterations per source were needed to obtain a stable map. In a few cases there was so little data that only a model with Gaussian components was fitted to the calibrated amplitude data.

All but the 1.3 cm data were re-mapped at the NRL using a combination of the Caltech and AIPS data reduction packages. The general structures for all sources were confirmed and in some cases the dynamic range of the maps was significantly improved due to improved calibration and model fitting the residual visibility data. In Paper II we present the final hybrid maps from which the individual source components were measured as well as a table of component parameters.

The errors are estimated conservatively as: 10% for the component flux densities and the source sizes; a fifth of the beam at the wavelength used (i.e. 0.04 mas at 1.3 cm, 0.09 mas at 2.8 cm, 0.2 mas at 6 cm, and 0.6 mas at 18 cm) for the component separations.

An inspection of the errors of the position angles of individual components or their separations that were measured from the maps, as well as a comparison with the position angles obtained from model fits to those read off from the corresponding maps resulted in an estimate of the error in the position angles of 20°.

2.3. X-ray observations

Observations with the IPC aboard the EINSTEIN X-ray observatory of the sources 0016 + 73, 0212 + 73, 0454 + 84, 0716 + 71, 1749 + 70, 1803 + 78, 1928 + 73, and 2007 + 77 were made starting in 1979. Early results have been reported in Biermann *et al.* (1981). The flux densities have been rederived using reprocessed data. The details of the observations will be presented elsewhere (Biermann *et al.*, in preparation). EXOSAT observations were made of the sources 0615 + 82 and 1150 + 81 as well as for some other sources (Biermann *et al.*, in preparation).

The HEAO-A1 survey (Wood *et al.*, 1984) was used to set upper limits to the flux densities of the remaining sources 0153 + 74, 0836 + 71, and 1039 + 81. The X-ray flux densities derived from the observations with the three different X-ray satellites for

Table 2. Summary of experiments. Dwingeloo: Radiosterrenwacht Dwingeloo, Netherlands; GRAS: George R. Agassiz Radio Station, Texas, USA; HAYSTACK: Haystack Observatory, Massachusetts, USA; Jodrell Bank: Nuffield Radio Astronomy Laboratories, Great Britain; Crimea: Simeis Radio Astronomy Station, Crimea, USSR; MPIfR: Max Planck Institut für Radioastronomie (100 m radiotelescope); NRAO: National Radio Astronomy Observatory, Green Bank, West Virgina, USA; NRL: Naval Research Laboratory, Washington, DC, USA; Onsala: Onsala Space Observatory, Sweden; OVRO: Owens Valley Radio Observatory, California, USA; Westerbork: Radiosterrenwacht, Westerbork, Netherlands

Epoch	Bandwidth (MHz)	Frequency (MHz)	Integration time (s)	Stations	Sources	Comments
1979.93	2	5010	240	MPIfR, HAYSTACK, GRAS, NRL, OVRO	All 13 sources but 1039 + 81	4 to 5 measurements per source over a range of 12 h
1980.11	2	5010	240	MPIfR, HAYSTACK, OVRO	1928 + 73, 2007 + 77	Scans of 20 min length switching between both sources for 12 h
1981.79	2	1666	360	Crimea, Dwingeloo, Jodrell Bank, MPIfR, Onsala, NRAO, NRL, OVRO	All 13 sources	Five 20 min scans per source over a range of 12 h
1982.95	2	4990	240	Jodrell Bank, MPIfR, Onsala Westerbork, NRAO, NRL, OVRO GRAS	1928 + 73, 2007 + 77	Scans of 15 min length switching between both sources for 12 h
1983.09	28	22235	180	MPIfR, Onsala, HAYSTACK, NRAO, OVRO	0212 + 73, 0454 + 84, 0615 + 82, 0836 + 71	Each pair was observed for 12 h for 13 min per hour and source. Scans of 13 min length, switching between four sources for 12 h. 0212 + 73 and 0836 + 71 were preferentially observed
1983.25	2	4990	240	MPIfR, HAYSTACK, NRAO, OVRO	0716 + 71, 0836 + 71 1039 + 81, 1150 + 81	
1983.10	2	10650	240	MPIfR, HAYSTACK, NRAO, OVRO	0016 + 73, 0212 + 73 1039 + 81, 1150 + 81	Both source pairs were observed for 12 h, switching between 2 sources. Scans of 15 min lengths
1983.92	2	4998	240	MPIfR, Westerbork, Jodrell Bank, Onsala, NRL, NRAO, HAYSTACK, OVRO	0153 + 74, 0212 + 73, 1803 + 78	Scans of 15 min length switching between 0153 + 74 and 0212 + 73 for 12 h. For 1803 + 78 same network but OVRO, full coverage, 12 h of observation

the sources in the sample are given in the last column of Table 4 (Paper II). It is important to note that the EXOSAT observations are most sensitive to absorption along the line of sight, since the instrument cuts off at 2 keV, while the other two instruments are sensitive to higher photon energies. Thus there are likely to be unknown systematic errors in the X-ray flux densities arising from unknown absorption outside our galaxy and unknown spectral index in the X-ray range. Here we have used the absorbing column density derived from H I measurements in our galaxy and an energy spectral index in the X-ray range of -0.5; for details see Biermann *et al.* (1981) and Biermann *et al.* (in preparation).

Table 3. General Source Structure[a]

Structure	Wavelength			
	18 cm	6 cm	2.8 cm	1.3 cm
Unresolved	3 (1)	–	–	–
Slightly resolved	2 (0)	3 (1)	2	–
Jet-like	8 (5)	10 (5)	2 (1)	4 (3)

[a] Figures in brackets correspond to BL Lac objects only

3. Results

3.1. General source structures

Classifying the different objects as unresolved, slightly resolved, or jet-like (two or more, aligned components or a single, heavily elongated Gaussian component), we can summarize their mas structure as given in Table 3. The figures in brackets correspond to BL Lac objects. In our sample their structure does not differ significantly from those of the quasars. At the higher frequencies, the sources were generally more resolved. All the sources consist of several components and appear to display asymmetric structures (with the possible exception of 1803 + 78).

The milliarcsecond source structure displayed by the S5-sample at 6 cm is typical of that displayed by compact extragalactic radio sources (see also Eckart, 1981). The structures in Table 3 are similar to those found by Readhead and Pearson (1981), who summarize the 6 cm structures of a similar sample of radio sources taken from the NRAO-MPIfR Strong Sources Surveys.

Since the overall radio spectra (at least for the quasars and BL Lacs – our sample does not contain any galaxies) and the radio through X-ray spectra – as far as measured – are similar for the sources of both samples, the statistical results provided by this paper can be taken as general for all extragalactic flat spectrum radio sources in the corresponding flux density range at 6 cm wavelength.

3.2. The arcsecond structures

All 13 sources have been observed with the VLA at 6 cm and 20 cm wavelength (Ulvestad *et al.*, 1981; Perley *et al.*, 1980; Johnston *et al.*, 1984). In addition we have reobserved 1928 + 73 at 20 cm wavelength using the VLA in C-configuration. With the MERLIN array we observed all sources but 1749 + 70 at 18 cm wavelength. In all cases the MERLIN data is consistent with the VLA data. In this paper we only summarize the global properties of the arcsecond structures of the sample.

With the exception of 0716 + 71, which exhibits about 50% of the total flux density in diffuse emission on opposite sides of the core (flux density ratio of the secondary components about 3:1), none of the sources show secondary components containing more than 10% of the flux densities of the primary components at wavelengths around 20 cm. Further significant emission from secondary arcsecond components is found in 0836 + 71 (Perley *et al.*, 1980: 10% at 20 cm and 2% at 6 cm) and 1928 + 73 (Johnston *et al.*, 1986, in preparation).

Weak evidence for emission from regions other than the central components is found by Perley (1982) for 1039 + 81, 1150 + 81, 1749 + 70 and 2007 + 77. No significant emission from secondary arcsecond components at dynamic range of 50:1 was found for the remaining 7 objects of the sample.

3.3. Component sizes and separations

Taking into account all the maps shown in Paper II at the various frequencies and resolutions, no source remains unresolved. Including resolved halo type components like in 0615 + 82, the number of secondary components varies from one to at least 9 (in the case of the complex jet in 1928 + 73).

After accounting for the known redshifts or their lower limits, the projected linear separations ($q = 0.05$, $H = 50\,\mathrm{km\,s^{-1}\,Mpc^{-1}}$) of the mas source components range from at least 2 pc (lower limit for the separation between the *A* and *B* components in 2007 + 77) to 124 pc (separation between the two compact components of 0153 + 74).

We note that the overall linear sizes of the compact emission at 1.6 and 5 GHz for the three sources which display the largest mas structures and have known redshifts are of the same order, although their redshifts are different (0153 + 74, $z = 2.34$, 124 pc; 0836 + 71, $z = 2.16$, 108 pc; 1928 + 73, $z = 0.36$, 113 pc).

3.4. Structural misalignments

Following Readhead *et al.* (1978) we expect a large fraction of these sources to show a significant misalignment between the mas and arcsec structure.

The largest misalignment occurs in the BL Lac object 0716 + 71. The change in position angle between the mas and the arcsec structure is at least 70°. The smallest misalignment is displayed by the source 0836 + 71 and is smaller than the error of 20° in measuring the position angle of the structure.

3.5. Identification of components

In order to investigate the radio spectra of individual source components and the kinematics of the sources, the individual source components must be identified at different wavelengths and epochs. Although only the relative positions of the source components are known, in all cases reasonable identifications of single components or groups of components could be made by comparing the source structures at different wavelengths and epochs, after taking into account the different dynamic ranges and resolutions of the maps. A table of the individual components is given in Paper II.

3.6. Spectral indices

We investigated the distribution of the spectral indices calculated between 18 cm and 6 cm wavelength. At these wavelengths we have maps and models of all the sample sources and most of the 18 cm components have counterparts at 6 cm. For the calculations we only used the most recent available 6 cm maps because these have a better dynamic range than the early measurements in 1979/80. Generally only clearly identified components or groups of components were used (see Table 3 in Paper II).

Corrections for resolution effects at 6 cm have been applied for the sources that contain almost all the total flux density in their 18 cm *VLBI* structure and/or have arcsec components of known flux density. The reliability of the spectral indices suffers from flux density variability of the sources between the 18 cm and 6 cm epochs, different resolutions, and different dynamic ranges. Even though the spectral indices for individual components are somewhat doubtful, we nevertheless think that the median spectral index values of the secondary and primary 18 cm components can be taken as representative for flat spectrum sources selected by similar criteria as for this sample. The errors on the median values were defined as half the interval that contains about $\frac{2}{3}$ of the values of the corresponding spectral index distribution. Figure 1 plots the number versus the spectral index for the primary and secondary components. The spectral indices for the primary 18 cm source components are in all cases

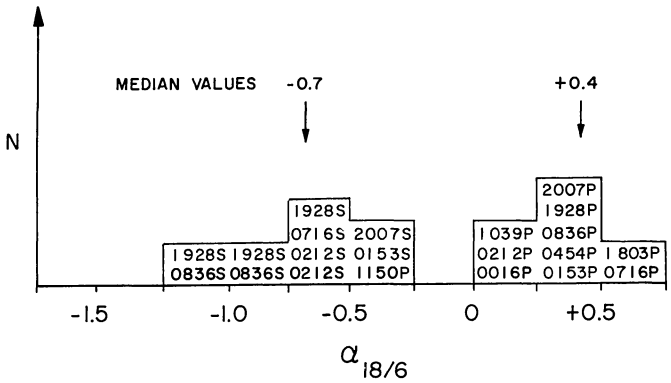

Fig. 1. The spectral index distribution between 18 cm and 6 cm wavelength. The spectral indices are calculated for the primary (*P*) and secondary (*S*) components of the 18 cm hybrid maps (see Table 3, Paper II)

but one (1150 + 81) inverted and result in a median value of $+0.4 \pm 0.2$. This indicates that the primary components are self-absorbed at 6 cm wavelength.

The spectral indices of the secondary components are less than 0 in all cases and have a median value of -0.7 ± 0.3. This indicates that the secondary components are optically thin at 18 cm wavelength, having a median spectral index that is in good agreement with the value of optically thin synchrotron sources of -0.7 (Moffet, 1975) observed elsewhere.

3.7. Decomposition of radio spectra

In all cases we can decompose the overall radio spectra of the sources into spectra of individual components. Figure 2 shows the decomposed spectra of 6 sources which exhibit the largest number of components or groups of components that are detected at different frequencies. Extrapolating the component spectra beyond the lowest and highest frequency where interferometer measurements were carried out and taking into account the shape of the overall radio spectra one can derive rough estimates (or limits) of the cut-off frequency ν_m and the corresponding flux density S_m. Furthermore the *VLBI* data provide approximate estimates of the component sizes θ_{VLBI}. Using the relationship

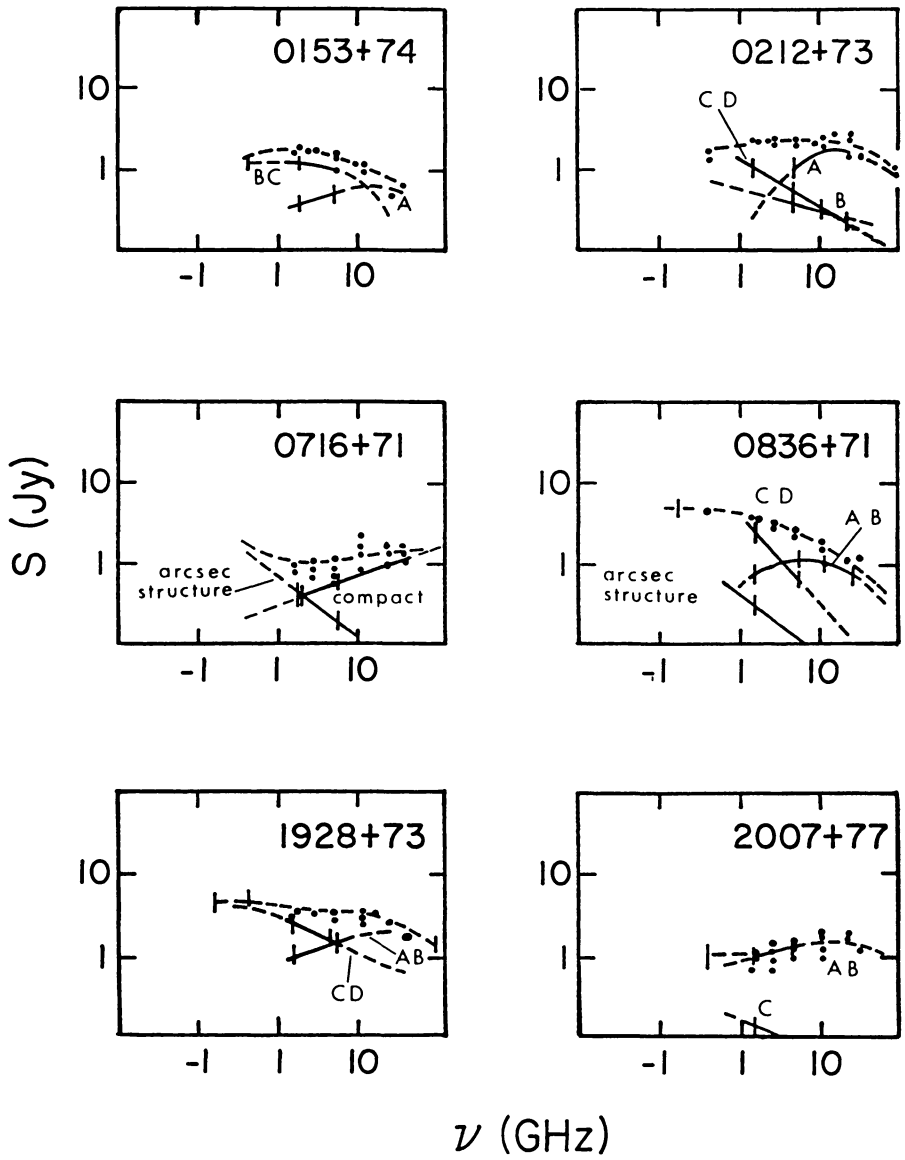

Fig. 2. Decomposition of the overall radio spectra of 6 sources into spectra of individual components. · Measurements of the multi-epoch radio spectrum. | VLB measurements of component spectra. ——— Interpolation of the multi-epoch radio spectrum. ------ Interpolation of the component spectrum

between the magnetic field strength B, the redshift z, S_m, ν_m, and θ_{VLBI} (Kellermann and Pauliny-Toth 1969):

$$\nu_m = f(\gamma) B^{1/5} S_m^{2/5} \theta_{VLBI}^{-4/5} (1+z)^{1/5}$$
$$f(\gamma) = 8 \quad \text{for } \gamma = 2 \tag{1}$$

we can calculate the magnetic field strength B' (using S_m, θ_{VLBI}, ν_m, z), cut-off frequency ν_m (using S_m, θ_{VLBI}, z and assuming $B = 10^{(-3\pm1)}$ G) and the component size θ (using S_m, ν_m, z and again assuming B as given before). For the sources of Fig. 2 this results in the values listed in Table 4. Obviously the estimated and calculated values are in good agreement and calculated magnetic field strengths are always larger than the value B_R corresponding to the energy of the 3 K background radiation at the given (or assumed) redshifts

$$B_R = 4(1+z)^2\, 10^{-6}\,\text{G}. \tag{2}$$

Unfortunately, this agreement is due mainly to the functional dependencies of the various quantities on the observables. The lack of large discrepancies does imply that ordinary synchrotron radiation from mostly homogeneous components is not ruled out as an emission mechanism for these sources.

3.8. *Kinematics*

For 8 of the 13 sources of the complete sample second epoch observations at 6 cm were made. The time difference between the epochs is about 2 to 4 years. Four of the sources (0153 + 74, 0716 + 71, 0836 + 71 and 1803 + 78) did not display significant changes in their component separations. It should be noted that of the four sources that show no discernible motions the two with known redshifts (0153 + 74 and 0836 + 71) have upper limits to any possible motion still in excess of any "typical" superluminal behaviour ($v/c \gtrsim 10$). For four of the sources (0212 + 73, 1150 + 81, 1928 + 73 and 2007 + 77) an increase in the angular distance D between their components was found. To convert the angular velocities $m = dD/dt$ (or their lower limits) into projected velocities in units of the velocity of light we used the following expression ($q = 0.05$, $H = 50\,\text{km s}^{-1}\,\text{Mpc}^{-1}$):

$$v(c) = \frac{3.8 \cdot 10^4\, \theta}{(1+z)t} \{0.05z - 0.95[(1+0.1z)^{1/2} - 1]\} \tag{3}$$

where θ is in mas and t in years.

Due to the fact that the BL Lacs do not appear to be extended on deep photographic plates and CCD images, a value of $z \geq 0.05$ was assumed for their redshift.

Under the assumption that the error on the amount of change in angular separation is less than 0.2 mas we can give upper limits for the transverse velocity of the stationary quasar structures and lower limits for the maximum possible projected velocities for the BL Lac structures. For all 8 sources we listed the quantities used to calculate the limits or definite values of the transverse velocities in Table 5. Table 5 summarizes positions of components for the 6 cm experiments. Columns 2 and 3 identifiy the two components for which the relative position is listed in columns 4 through 9 for the various epochs. Columns 10–11 list the apparent motion in mas/yr, while column 12 lists the apparent velocity.

In the cases of the BL Lac objects 0212 + 73 and 2007 + 77 the observed angular motions results in an apparent velocity greater than the speed of light if the redshifts are larger than 0.1 and 0.05, respectively. For the quasar 1150 + 81, the apparent projected velocity at the redshift of $z = 1.25$ is 10c.

1928 + 73 is discussed in Eckart *et al.* (1985). We note that due to the poor coverage at the first epoch for the other candidates (0212 + 73, 1150 + 81 and 2007 + 77) the evidence for structural changes is not as strong as it is for 1928 + 73. Observing programs to search for structural changes in the remaining 3 cases are underway.

4. Discussion

The expression given by Marscher (1983) for the expected Compton flux density S_{IC} in the standard Synchrotron-Self-Compton

Table 4. Physical parameters of the components

Source	z	Comp.	ν_m	S_m [Jy]	θ' [mas]	θ [mas] *VLB*	B' [G]	ν'_m [GHz]	B_R [10E-5 G]
0153 + 74	2.33	*A*	20	0.8	0.4 . . . 0.12	< 0.25	< 0.2	> 5	4
		BC[b]	1	1.2	2 . . . 7	< 10	< 0.06	> 0.3	
0212 + 73	0.1[a]	*A*	15	1.9	0.06 . . . 0.20	< 0.3	< 0.05	> 5	0.5
		B	< 1.6	> 0.4	> 0.5	< 0.8	< 7 10E-4	> 1	
		C[b]	< 1.6	> 0.6	> 0.6	< 2	< 12 10E-3	> 0.6	
		D[b]	< 1.6	> 0.6	> 0.6	< 2	< 12 10E-3	> 0.6	
0716 + 71	0.1[a]	*ABC*	> 22	> 1	< 0.1	< 0.5	< 9	> 2	0.5
0836 + 71	2.16	*AB*	5	1.4	0.3 . . . 0.9	< 1	< 15 10E-3	> 2	4
		C	< 1.6	> 1.4	> 1.2	< 2.4	< 17 10E-3	> 0.9	
		D[b]	< 1.6	> 1.9	> 1.3	< 10	< 0.3	> 0.3	
1928 + 73	0.36	*AB*	20	2	0.05 . . . 0.16	< 2	< 280	> 1	0.7
		C to *I*	< 1.6	> 2.6	> 1.3	< 20	< 6	> 0.2	
2007 + 77	0.1[a]	*AB*	15	2	0.06 . . . 0.2	< 2	< 80	> 1	0.5
		C	< 1.6	> 0.2	> 0.35	< 4	< 2	> 0.2	

[a] Estimated redshift

[b] Estimates of S taken from Fig. 2, angular diameters from Table 2, Paper II

Table 5. Summary of relative positions of components

Source	Reference comp.	Secondary comp.	Separation at		Epoch [mas]					mas/yr	v/c	z
			1979.93	1980.11	1980.72	1982.95	1983.25	1983.92				
0153 + 74	C1	C2	10.2 ± 0.2					10.3 ± 0.3		< 0.09	< 12	2.33
0212 + 73	C1	C2	1.0 ± 0.1					1.4 ± 0.1		0.10 ± 0.04	> 1 for	> 0.1
0716 + 71	C1	C2	1.3 ± 0.2				1.6 ± 0.3			< 0.11	< 1 at	0.1
0836 + 71	C1	C2	3.0 ± 0.2				2.9 ± 0.4			< 0.13	< 17	2.16
1150 + 81	C1	C2	1.35 + 0.05				1.76 ± 0.11			0.12 ± 0.04	10 ± 3	1.25
1803 + 78	C1	C2	1.2 ± 0.3					1.2 ± 0.2		< 0.09	< 0.5 at	0.05
1928 + 73	C1	C2			< 0.2	1.15 ± 0.10			> 0.4			
	C1	C3			1.98 ± 0.12	3.45 ± 0.16			0.66 ± 0.09			
	C1	C4			3.59 ± 0.18	4.87 ± 0.26			0.57 ± 0.14	0.60 ± 0.16	18 ± 5	0.36
	C1	C6, C7			8.25 ± 0.27	9.54 ± 0.24			0.58 ± 0.16			
	C1	C9			16.2 ± 0.2	6.87 ± 1.22			0.30 ± 0.55			
2007 + 77	C1	C2		0.76 ± 0.08		1.50 ± 0.2				0.26 ± 0.08	> 1 for	> 0.05

model can be written as:

$$S_{IC} = f(\alpha) T_B^{3-2\alpha} S \nu^{1-\alpha} E^{\alpha} \left(\frac{1+z}{D} \right)^{2(2-\alpha)} \quad (4)$$

where S is the radio flux density in Jy, ν the radio frequency in GHz, θ is the width (at half maximum) of the observed compact component in mas, E the X-ray Energy in keV (we will use 1 keV as reference), and S_{IC} the X-ray flux density in μJy, D is the relativistic boosting factor (which we set to unity) and z the redshift. The brightness temperature is given in units of 10^{12} K by

$$T_B = 1.22 \frac{S}{\nu^2 \theta^2}. \quad (5)$$

From our data the optically thin spectral index – which has to be used here – is in the range of α -0.4, -0.7 and -1.0, for which values of $f(\alpha)$ are 3.9, 1.0 and 0.31 respectively.

Table 4 in Paper II gives the brightness temperature, the result of applying the above expression for S_{IC}, and the observed X-ray flux density at 1 keV. The uncertainty in the spectral index translates into an uncertainty of the expected inverse Compton flux density of about a factor $\lesssim 100$. We find an excess of expected over observed X-ray emission for the sources 0016 + 73 and 0836 + 71. Such an excess is often used as supporting evidence to suggest relativistic bulk motion, which for certain orientations of the source axis would be visible as superluminal expansion.

Further, considering the brightness temperature of the various components visible at different frequencies, we note that for equally good baseline coverage, the brightness temperature (here always lower limits!) is independent of frequency, in agreement with the theoretical model of Blandford and Königl (1979). Since the various self-absorbed components add up to produce a flat spectrum, we can speculate whether this property continues into the mm-wavelength range as yet unobserved by *VLBI* for sources known to have flat spectra to high frequencies. Since our selection criterion was flat radio spectra, we can therefore speculate on the properties of the compact components dominant in the mm range. One source in our sample, 1803 + 78, is listed in the IRAS point source catalogue (IRAS, 1985) and is thus known to have a nearly flat spectrum into the far-infrared region. Assuming therefore, that 1) the brightness temperature is independent of frequency (i.e. for the different compact components dominant at different frequencies), 2) that the flux density of the compact components is not too different from the values at lower frequencies, and 3) that the most compact component exists at least at 300 GHz, we can extrapolate the expected inverse Compton flux densities S_{IC} to give the extrapolated inverse Compton flux densities S_{IC}^{*} (see Table 4 in Paper II). S_{IC}^{*} is then just S_{IC} multiplied by $(300/\nu)^{1.7}$. By requiring a factor of ten discrepancy, we now find, on these speculative grounds, suggested bulk relativistic motion is found for all sources in the sample except 1749 + 70 and 0716 + 71. For 1749 + 70 the *VLBI* data are not of the same quality as the rest of the sample, and so any conclusion has to be looked at with caution. For 0716 + 71, as for the other BL Lacs in the sample, we have used the conservative low redshift of 0.05; had we used, say, the average value of the redshift for the quasars in our sample, 1.3, all the expected inverse Compton flux densities would be larger by a factor of 69. Hence it is rather likely that 0716 + 71 would also have a severe discrepancy of expected over observed X-ray emission.

Combining these results with those of the direct observation of superluminal motion in four sources in our sample, we conclude that our small, but complete sample has a high probability of all its sources being relativistic. More *VLBI* epochs of the frequencies already observed, higher frequency *VLBI*, and more sensitive X-ray data are required to actively pursue these questions.

5. Conclusion

The thirteen extragalactic sources of the S5 survey with flux densities ≥ 1 Jy at 4990 MHz at the epoch of the S5 survey have been mapped with milliarcsecond resolution at 18 and 6 cm wavelengths. All sources appear to display multiple components which are dominated in flux density at 6 cm by a core component which is self-absorbed at 18 cm. The other features appear to have optically thin spectra. Comparison of the observed to predicted X-ray flux densities indicates that many of these sources should display apparent superluminal motion. Indeed four sources 0212 + 73, 1150 + 81, 1928 + 73 and 2007 + 77 show changes in their radio structure at 6 cm between mapping epochs which can be interpreted as apparent superluminal motion.

The individual maps and extensive tabular material regarding the 13 sources are given in Paper II.

Acknowledgement. We would like to thank the numerous colleagues who have helped in various aspects of this work. Special thanks are due to Drs. I. Pauliny-Toth, R.W. Porcas and J.A. Zensus for critical discussions. We also wish to thank the staff at the various observatories who have made this project possible, and, in particular, Mr. H. Blaschke, Mr. U. Stursberg and Mr. H. Lüdecke, for their patient work with the Mk II and Mk III processors.

References

Arp, H., Sulentic, J.W., Willis, A.G., de Ruiter, H.R.: 1976, *Astrophys. J.* **207**, L13

Biermann, P., Fricke, K., Johnston, K.J., Kühr, H., Pauliny-Toth, I.I.K., Strittmatter, P.A., Urbanik, M., Witzel, A.: 1982, *Astrophys. J.* **252**, L1

Biermann, P., Duerbeck, H., Eckart, A., Fricke, K., Johnston, K.J., Kühr, H., Liebert, J., Pauliny-Toth, I.I.K., Schleicher, H., Stockman, H., Strittmatter, P.A., Witzel, A.: 1981, *Astrophys. J.* **247**, L53

Blandford, R.D., Königl, A.: 1979, *Astrophys. J.* **232**, 34

Clark, B.G.: 1973, *Proc. of the* IEEE, **61**, No. 9

Crane, P.D., Price, R.M.: 1976, *Astrophys. J.* **207**, L21

Eckart, A.: 1981, Diploma thesis, Univ. of Münster

Eckart, A., Hill, P., Johnston, K.J., Pauliny-Toth, I.I.K., Spencer, J.H., Witzel, A.: 1982, *Astron. Astrophys.* **108**, 157

Eckart, A., Witzel, A.: 1983, Proc. of the IAU *Symp.* No. 110, 65

Eckart, A., Witzel, A., Biermann, P., Pearson, T.J., Readhead, A.C.S., Johnston, K.J.: 1985, *Astrophys. J.* **296**, L93

Eckart, A., Witzel, A., Biermann, P., Johnston, K.J., Simon, R., Schalinski, C., Kühr, H.: 1986, *Astron. Astrophys. Suppl.*, (in press) (Paper II)

IRAS, point source catalogue: 1985, Expl. Suppl., eds. Reichman, C.A., Neugebauer, G., Habing, H.J., Clegg, P.E., Chester, T.J.

Johnston, K.J., Biermann, P., Eckart, A., Kühr, H., Strittmatter, P.A., Strom, R.G., Witzel, A., Zensus, A.: 1984, *Astrophys. J.* **280**, 542

Kellermann, K.I., Pauliny-Toth, I.I.K.: 1969, *Astron. J.* **155**, L71

Kühr, H., Witzel, A., Pauliny-Toth, I.I.K., Nauber, U.: 1981, *Astron. Astrophys. Suppl.* **45**, 367

Kühr, H., Johnston, K.J., Odenwald, S. and Adlhoch, J.: 1986a, *Astrophys. J.* (submitted)

Kühr, H., Liebert, J., Strittmatter, P.A.: 1986b, (in preparation)

Marscher, A.P.: 1983, *Astrophys. J.* **264**, 296

Moffet, A.T.: 1975, Stars and Stellar Systems *IX*, 211

Perley, R.A.: 1982, *Astron. J.* **87**, 859

Perley, R.A., Fomalont, E.B., Johnston, K.J.: 1980, *Astron. J.* **85**, 649

Readhead, A.C.S., Cohen, M.H., Pearson, T.J., Wilkinson, P.N.: 1978, *Nature* **276**, 768

Readhead, A.C.S., Pearson, T.J.: 1981, *Proc. of the* IAU *Symp.* No. 97, 279

Rogers, A.E.E., Cappallo, R.J., Hinteregger, H.F., Levine, J.I., Nesman, E.F., Webber, J.C., Whitney, A.R., Clark, T.A., Ma, C., Ryan, J., Corey, B.E., Counselman, C.C., Herring, T.A., Shapiro, I.I., Knight, C.A., Shaffer, D.B., Vandenberg, N.R., Lacasse, R., Mauzy, R., Rayhrer, B., Schupler, B.R., Pigg, J.C.: 1983, *Science* **219**, 51

Ulvestad, J., Johnston, K.J., Perley, R., Fomalont, E.: 1981, *Astron. J.* **86**, 1010

Witzel, A., Johnston, K.J.: 1982, Abhandlungen aus der Hamburger Sternwarte, Band X, Heft 3, eds. Argue, A.N. and de Vegt, C.

Wood, K.S., Meekins, J.F., Yentis, D.J., Smathers, H. W., McNutt, D.P., Bleach, R.D., Byram, E.T., Chubb. T.A., Friedman, H., Mediav, M.: 1984, *Astrophys. J.* **56**, 507